Anal. Bioanal. Electrochem., Vol. 14, No. 4, 2022, 432-443

Analytical & Bioanalytical Electrochemistry

2022 by CEE
www.abechem.com

Full Paper

Electrochemical Detection of Uric Acid by using NiO Nanoparticles

K. Gangadhara Reddy,[1] Sathish Reddy,[2,*] B.E. Kumara Swamy,[3,*] Mohan Kumar,[4] K. N. Harish,[5] C. S. Naveen,[6] G. Ranjith Kumar,[7] and T. Aravinda[8]

[1]*Department of Chemistry, S.V.U. College of Sciences, Sri Venkateshwara University, Tirupati-517502, Andhra Pradesh, India*
[2]*School of Chemical Science, School of Applied Science, REVA University, Bangalore, 560064, India*
[3]*Department of Industrial Chemistry, Kuvempu University, Shankaraghatta, 577204, Shimoga, India*
[4]*Department of Chemistry, PES Institute of Technology and Management, Sagar Road, Guddada Arakere, Kotegangoor-577204, Shivamogga, India*
[5]*Department of Chemistry, Dayananda Sagar College of Engineering, Shavige Malleshwara Hills, Kumaraswamy Layout, Bengaluru, 560078, India*
[6]*Department of Physics, School of Engineering, Presidency University, Bengaluru-560064, India*
[7]*Department of Physics, School of Applied Science, REVA University, Bangalore, 560064, India*
[8]*Department of Chemistry, Nitte Meenakshi Institute of Technology, Bangalore-560064, India*

*Corresponding Author, Tel.: +919353808562
E-Mails: sathish.reddy@reva.edu.in and gnsathishreddy@gmail.com (Sathish Reddy)

Received: 23 July 2021 / Received in revised form: 15 April 2022 / Accepted: 18 April 2022 / Published online: 30 April 2022

Abstract- High and low-level concentrations of uric acid (UA) lead to several diseases and physiological disorders. A simple method or sensor is required for the detection of UA. In this work, we have prepared a NiO nanoparticles/ carbon paste electrode (NiONPs/CPE) as an electrochemical sensor and applied it for the detection of UA. Electrochemical parameters such as the effect of pH, scan rate, and concentration were studied. The obtained results represent the excellent electrocatalytic activity of NiONPs/CPE with a diffusion-controlled electrode process. The electrocatalytic process was pH-dependent with a slope of 59 mV/pH. Peak current increased linearly with the increases in UA concentrations. The detection limit was found to be 0.1 μm for the linear range from 0.19 μM to 49 μM. The NiONPs/CPE electrodes exhibited good sensitivity for the detection of UA. As a result, this work is expected to be used for the development of a sensor for the detection of UA.

Keywords- Nickel oxide nanoparticles; Uric acid; Modified carbon paste electrode; Electrochemical sensor

1. INTRODUCTION

Nickel oxide (NiO) has a cubic lattice structure. It has a variety of uses, such as catalysis [1], gas sensors [2], magnetic materials [3], electrochromic films [4], and battery cathodes [5]. Because of its quantum size effect and surface effect, NiO has become an interesting topic in the new area of research. Nano-sized NiO enhanced its properties more than the bulk NiO particles.

Uric acid (2,6,8-trihydroxypurine, UA) is a heterocyclic organic compound with the chemical formula $C_5H_4N_4O_3$. Uric acid is a by-product of the metabolic breakdown of purine nucleotides and it is a normal component of urine. Uric acid (UA) is a product of purine nucleotides and it is insoluble in water [6]. It is distributed in the urine, blood, serum, and kidneys [7]. In a healthy person, the normal concentration of UA is in serum (240–520 μM), blood (120–450 μM), and urine (1.2–4.4 μM) [8,9]. Variations in UA concentration lead to various diseases and disorders. A high-level UA concentration can lead to diseases like goat, Lesch-Nyhan syndrome, hyperuricemia, and renal failure [10,11]. A low-level concentration of UA may cause such conditions as copper toxicity, molybdenum deficiency, and multiple sclerosis. A very low concentration of UA may cause Wilson's disease and Fanconi diseases [12].

Several studies [13,14] have found that variations in UA concentration in serum cause cardiovascular disease. UA has multifunctional benefits, and it is an important biomolecule antioxidant in blood plasma. Thus, it is required simple, accurate, and reliable for the detection of UA concentration. Several methods, such as colorimetric [15], spectrofluorimetric enzymatic [16], chemiluminescence [17], and chromatography technique [18], have been used for the detection of UA. The electrochemical methods have been shown to be less costly, eco-friendly, time-consuming, and selective for the detection of UA. The most widely adopted electrochemical method for the detection of UA uses the enzymatic approach method [19]. The uricase enzyme reacts with UA and produces hydrogen peroxide, which is detected by

electrochemical methods. However, an enzymatic method has fatal problems, such as the low stability of enzymes, high cost, and the fact that the detection is indirect [19]. Several studies have reported nonenzymatic methods for the detection of UA.

Several kinds of literature reported on NiO nanosized particle modifier electrodes for the investigation of uric acid because research advancements in sensor technology have been focused on smart nanoscale particles for the preparation of sensors. Several methods have been adopted to synthesize nanosized NiO particles. However, only a few studies on NiO-based sensors have been published, such as S. Reddy et al. [20], who developed a NiO nanoparticle-based sensor for the detection of dopamine (DA), explaining that NiO nanoparticles have a high surface area, which increases electrocatalytic activity with an increased lower detection limit and sensitivity. Similarly, Hang Yue et al. investigated whether NiO-rGO has a high sensitivity for detecting UA in the presence of interference because NiO-rGO enhances the surface active area, electrostatic attraction, and electron transfer rate [21]. In addition, R.A. Soomro et al. reported that NiO nanoparticles enhanced lower detection, high sensitivity, and high linear range for the detection of glucose [22]. Moreover, S. Reddy et al. reported that NiO/ZnO hybrid nanoparticles showed good sensing properties for the detection of DA and UA because nanoparticles enhanced electrocatalytic activity [23]. Furthermore, A.S. Chang et al. have shown silky Co_3O_4 nanostructures enhance the electrocatalytic activity for the detection of UA. Because Co_3O_4 nanoparticles enhance the surface area of the electrode [24].

However, most reported electrodes showed a lower detection limit in macro-to micro-level concentration, which is not sensitive enough for the detection of UA. In addition, there is very little literature reported on the electrochemical detection of UA using NiO nanoparticles (NiO NPs). Moreover, already been reported that a small amount of NiO is dispersed uniformly over a conducting material, which increases the surface area and leads to increased electrical conductivity and ionic transport throughout the internal volume of the electrode [20]. Therefore, in this work, we have prepared NiO NPs by the co-precipitation method and characterized them. For modified carbon paste electrodes, NiO NPs were used. At a physiological pH of 7.4, NiO NPs-based carbon paste electrodes (NiO NPs/CPE) were applied for the electrochemical investigation of uric acid. The obtained results exhibited good electrocatalytic activity for the detection of uric acid from lower to higher concentrations of UA (0.1 μM to 49 μM).

2. MATERIALS AND METHODS

2.1. Apparatus

The NiO nanoparticles (NiO NPs) were characterized by using several methods. By ultrasonication of NiO NPs in an ethanol solution, UV-visible spectra were taken from the UV–VIS spectrophotometer (Perkin Elmer) by ultrasonication. Philips X-ray diffractometer

equipment with Cu-K radiation (l= 1.5438 A^o) was used to record the XRD patterns of NiO NPs. The NiO NPs images were taken by using a scanning electron microscope (JEOL JSM-848) and transmission electron microscopy (a JEOL 2000 Fx-II transmission electron microscope from Oxford Instruments).

Voltammetry experiments were conducted using the CHI model 660c connected to a computer, which was used for electrochemical measurement and analysis. A three-electrode cell was used throughout the experiments, with a saturated calomel electrode (SCE) as a reference electrode, a platinum wire as a counter electrode, and a CPE or NiO NPs /CPE (3.0 mm in diameter, homemade cavity) as a working electrode.

2.2. Preparation of NiO nanoparticles (NiO NPs)

In a typical experiment, solution-A was prepared using 0.12M CH_3COOH, 0.06M $NiSO_4.6H_20$ in distilled water, and solution-B was prepared using 100 ml of absolute C_2H_5OH and 0.18M NaOH in distilled water. The solution-A was added slowly to solution B with continued stirring. The $Ni(OH)_2$ precipitate was filtered through filter paper (Whatman grade-41) and dried for about 1 hour at 80 °C. The dried $Ni(OH)_2$ precipitate was placed in a silica crucible and calcinated for approximately 3 hours at 400 °C. The resultant NiO NPs were washed with ethanol three to four times to remove impurities.

2.3. Chemicals and Solutions

Graphite powder was purchased from Merck chemicals. Silicon oil, uric acid, and sodium hydroxide were purchased from Himedia chemicals. Uric acid (UA) is acidic in nature and soluble in alkaline solution. All chemicals were of analytical grade with high purity. The double-distilled water was used for all the measurements. Phosphate buffer (PBS) (0.2 M) was prepared with 0.2 M sodium dihydrogen phosphate (NaH_2PO_4) and 0.2M disodium hydrogen phosphate (Na_2HPO_4).

2.4. Preparation of carbon paste electrode (CPE) and NiO NPs based carbon paste electrode (NiO NPs/CPE)

The carbon paste electrode (CPE) was prepared by mixing 20% silicon oil with 80% graphite powder in an agate mortar for approximately 30 minutes. The homogeneous carbon paste was packed into the 3 mm diameter cavity of the carbon paste electrode and smoothed using soft paper. The electrical contact was provided by a copper wire connected to the carbon paste at the end of the tube. The NiO NPs/ carbon paste electrode ((NiO NPs/CPE)) was made by adding different weights of NiO NPs (5, 10, 15, 20, and 25 mg) to a mixture of silicon oil (20%) and graphite powder (80%).

3. RESULTS AND DISCUSSION

3.1. Characterization

The XRD pattern of NiO NPs is shown in Figure 1. All the peaks are well-matched to the face center cubic structure of NiO (JCPDS PDF, no. 780429) with high crystallinity. The XRD pattern of the NiO NPs sample was observed to have no impurity peaks, which indicates the high purity of the NiO NPs, and the crystallite sizes of NiO NPs were found to be ~50 nm, which was determined by using Debye Scherrer's formula.

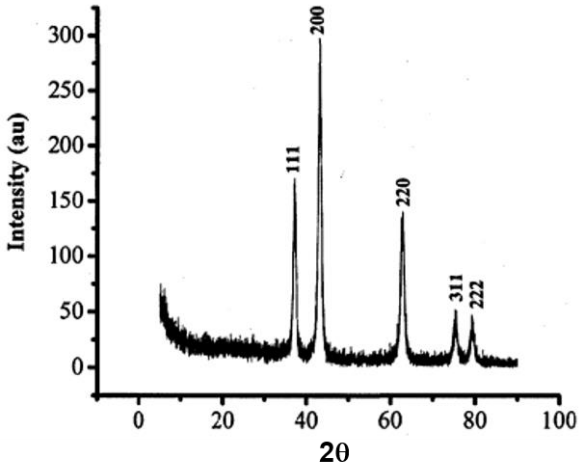

Figure 1. XRD pattern of NiO nanoparticles

The infrared absorption (IR) spectrum of the NiO NPs displays in Figure 2. A broad peak at around 3404 and 1632 cm^{-1} was due to H-OH stretching. Peaks at 1108, and 420 cm^{-1} are due to Ni-0 stretching.

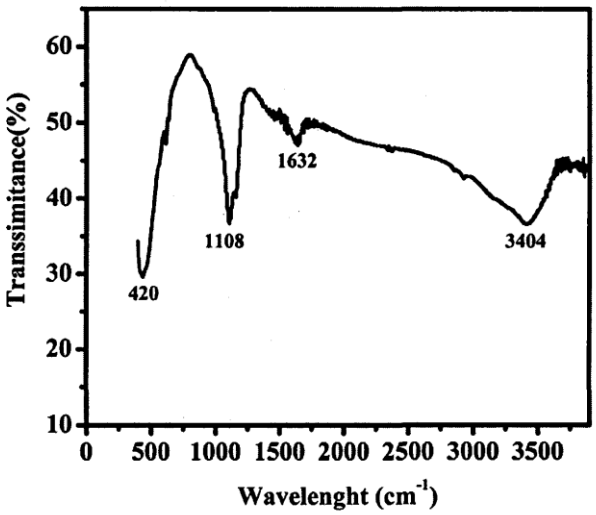

Figure 2. IR spectra of NiO Nanoparticles

The UV-Visible absorption spectrum of the NiO NPs dispersed in ethanol solution shows a sharp absorption peak of approximately 306 nm as shown in Figure 3. The obtained UV-visible absorption spectra for NiO NPs show a good blue shift.

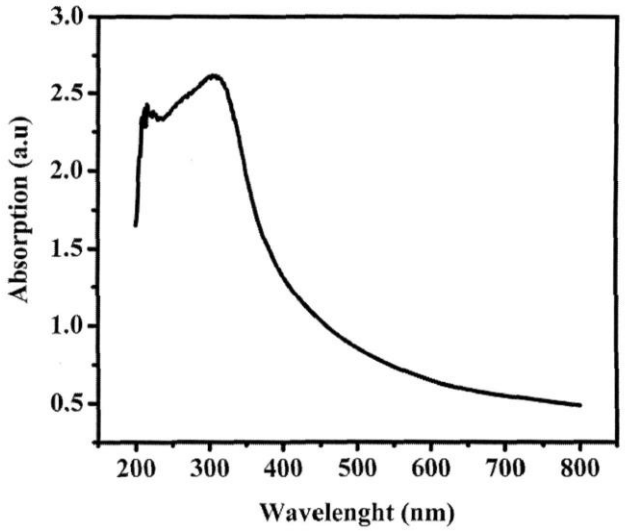

Figure 3. UV-Visible spectra of NiO Nanoparticles

The surface morphology of the samples was examined by SEM as shown in Figure 4. The SEM images clearly show irregular shapes having ~50-60% of ~50-60 nm, ~15-20 % of ~100 nm, ~10-15% of ~200nm, and ~10% of ~300-400nm. NiO NPs are irregularly and non-uniformly distributed have been observed.

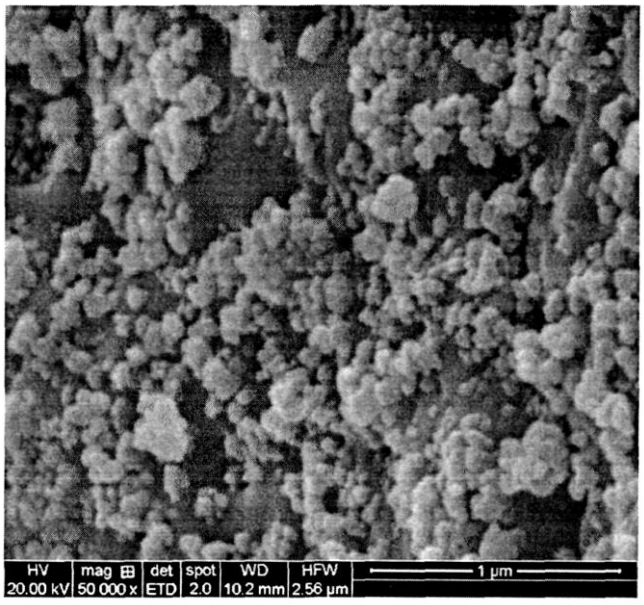

Figure 4. SEM image of NiO nanoparticles

3.2. Effect of NiO NPs (NiO nanoparticles) on peak current and peak potential

In order to select and optimize NiO NPs/CPE, cyclic voltammetry (CV) was scanned for different weights of NiO NPs/CPEs with a UA concentration of 1 mM in phosphate buffer solution (0.2 M PBS) at pH 7.4 and at a scan rate of 100 mVs^{-1}. The NiO NPs/CPE comprising 20 mg of NiO NPs in a CPE is more active with decreased peak potential and increased peak current than the bare CPE (0), 5, 10, 15, and 25 mg of NiO NPs. The graph Figure 5 (-■-) shows the relation between anodic peak current (I_{pa}) Vs concentration of NiO NPs in CPE. Similarly, the graph in Figure 5 (-●-) shows the relationship between the anodic peak potential (E_{pa}) and the concentration of NiO NPs in CPE. The optimized NiO NPs/CPE anodic peak potential and anodic peak current were found to be 0.31V and 130 μA, respectively. The anodic peak potential and anodic peak current of the CPE were found to be 0.39 V and 52 mA, respectively. This indicates that optimized NiO NPs/CPE (i.e., 20 mg NiO NPs in CPE) exhibited good sensitivity and electrocatalytic activity for the detection of UA. Therefore, optimized NiO NPs/CPE is applied for further electrochemical studies and detection of UA.

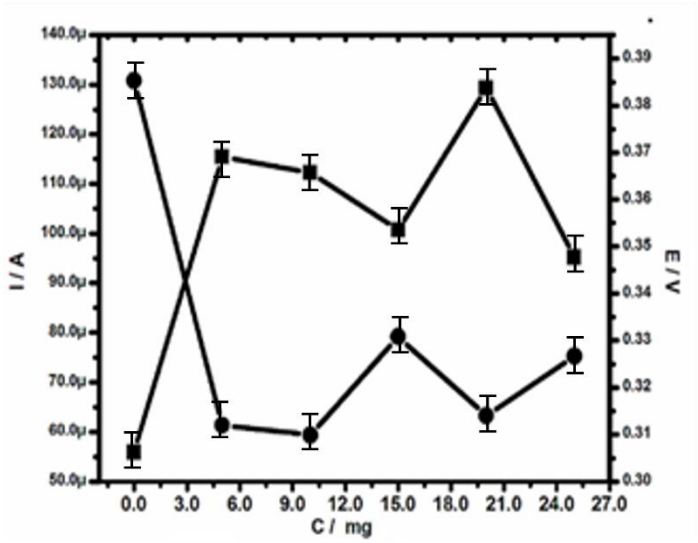

Figure 5. Effect of NiO NPs concentration in CPE on anodic peak current (I_{pa}), and anodic peak potential (E_{pa}) for 1 mM UA in 0.2M phosphate buffer solution with scan rate 100 mVs^{-1}

3.3. The response of UA at the CPE, and NiO NPs/CPE.

Figure 6 displays cyclic voltammogram responses of 0.1 mM UA in 0.2 M PBS (phosphate buffer solution) at pH 7.4 with a scan rate of 100 mV/s for CPE and NiO NPs/CPE. At CPE, oxidation peak potential occurs at 0.380 V, and for NiO NPs/CPE, oxidation peak potential occurs at 0.310 V, with a significant enhancement in peak currents. The reduction of oxidation peak potential and enhancement of peak current exhibits the excellent electrocatalytic activity and current sensing property of NiO NPs/CPE. The probable mechanism is that NiO NPs

expose more surface-active area for hydrogen bonding with UA, which activates UA to undergo very fast oxidation.

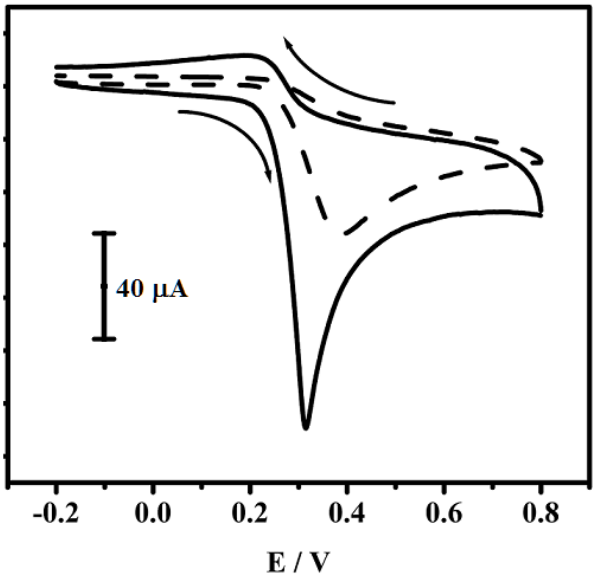

Figure 6. Cyclic voltammogram of 0.1 mM UA at the solid line for NiO NPs/ CPE and at the dotted line for CPE

3.4. Effect of pH

Figure 7 displays the cyclic voltammogram response of 1 mM UA in 0.2 M PBS (phosphate buffer solution, pH 5.5 to 8.0) at the NiO NPs/CPE. Peak current and peak potential were changed by a change in the pH of the electrolytic solution. Electrocatalytic activity depends on the pH of the electrolytic solutions. It can be determined by measuring peak current and potential. The NiO NPs/CPE electrocatalytic activity in different pH (5.5 to 8.0) electrolytic solutions are displayed in Table.1. It shows that increasing the pH of an electrolytic solution shows decreased peak current and peak potential. Figure 8 shows graphs of I_{pa} (A) and E_{pa} (V) versus pH of electrolytic solution for NiONPs/CPE. The anodic peak potential (E_{pa}) for the oxidation of UA decreased with an increase in the pH of the electrolytic solution. The E_{pa} of UA is shifted to a negative side potential with a slope of -57 mV/pH. The results suggest that equal electron transfer accompanied by equal proton transfer occurred.

Table 1. The electrocatalytic activity of the NiO NPs/CPE at different pH electrolytic solution

pH	E_p (V)	I_p (µA)
5.5	0.402	41.33
7.0	0.314	31.59
8.0	0.257	17.07

.

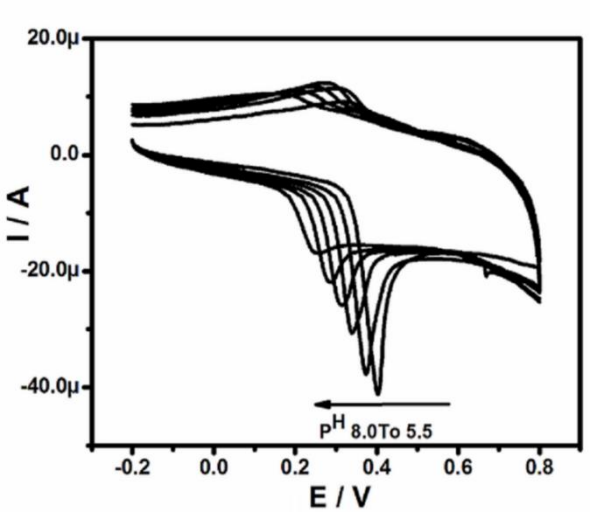

Figure 7. Series of cyclic voltammograms obtained for NiO NPs/CPE in different pH 0.2 M phosphate buffer solutions (PBS) at a scan rate of 100 mV/s

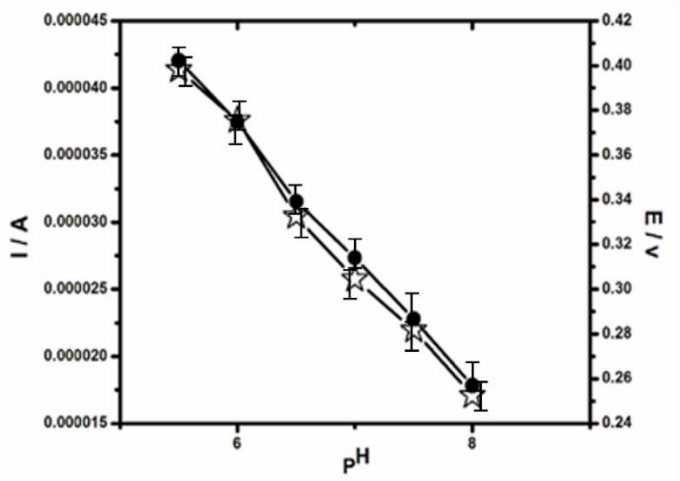

Figure 8. Different pH versus anodic peak potential (E_{pa}) (-●-) and anodic peak current I_{pa} (-☆-) for 1.0 mM UA in 0.2 M PBS electrolytic solutions at a scan rate of 100 mV/s for NiO NPs/CPE

3.5. Effect of scan rate

As shown in Figure 9, the cyclic voltammograms (CVs) of NiO NPs /CPE for 1 mM UA in 0.2 M PBS at pH 7.4 are dependent on the various scan rates. The effect of scan rates (50–1000 mVs^{-1}) on UA by cyclic voltammetry showed an increase in the peak current with an increase in scan rates. In a linear graph of the square root of scan rate ($n^{1/2}$) versus anodic peak (I_{pa}), I_{pa} was shown with a good correlation coefficient, R^2=0.99, as shown in Figure 10. This linearity graph shows a diffusion-controlled electrode process.

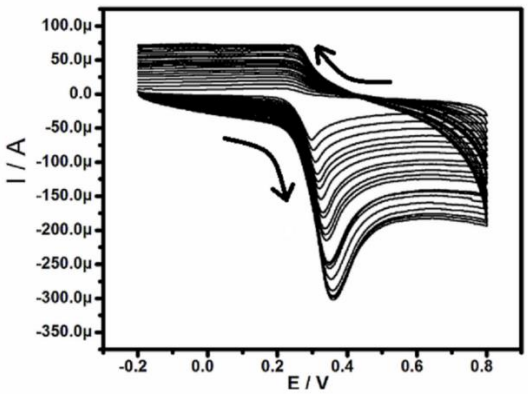

Figure 9. Series of cyclic voltammogram obtained for NiO NPs/CPE in 0.2 M PBS solution at pH 7.4, scan rate from 50 mVs^{-1} to 1000 mVs^{-1}

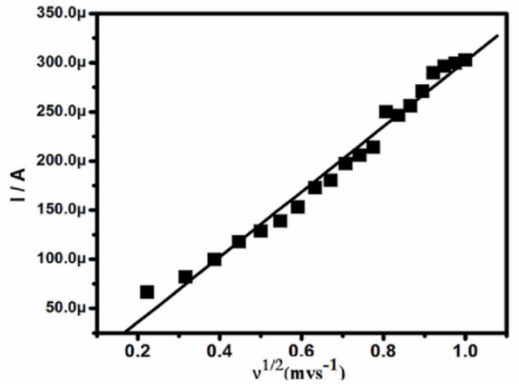

Figure 10. Graph of (I_{pa}) anodic peak current versus $n^{1/2}$ square root of scan rate for 1 mM UA in 0.2 M PBS (pH 7.4) for NiO NPs /CPE

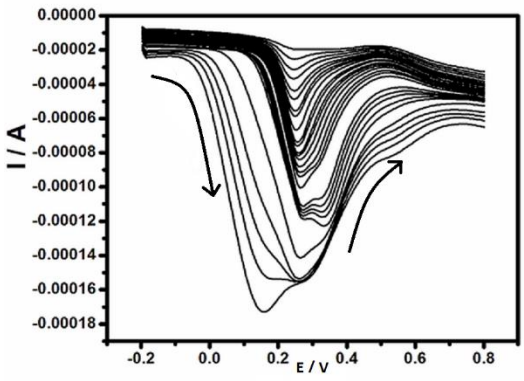

Figure 11. shows a differential pulse voltammogram (DPVs) of UA varying from 0.192 µM to 9200 mM in 0.2M PBS at pH 7.4. for NiO NPs/CPE

3.6. Effect of Concentration of UA

Figure 11 displays the (DPV) differential pulse voltammograms at NiO NPs/CPE for a concentration of UA varying from 0.192 µM to 9200 mM in 0.2M PBS at pH 7.4. The peak current increases linearly with the increasing UA concentration. Figure 12 displays the good

linearity between I_{pa} and UA concentration (0.192 μM to 9200 mM), the linear equation as shown in the graphs (Figure 12). The (LOD) lower detection limit for the lower linear range region was found to be 0.1 mM for NiO NPs/CPE, it showed better than the previous report [23].

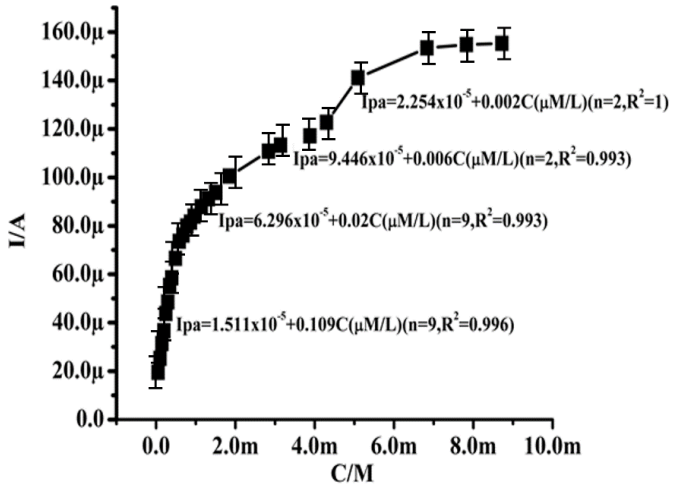

Figure 12. Graph of I_{pa} anodic peak current versus UA concentration for NiO NPs/CPE in 0.2 M PBS at pH 7.4.

4. CONCLUSIONS

A Nio nanoparticle was prepared and characterized. NiO nanoparticle-based electrochemical sensing applications were studied. NiO NPs/CPE exhibit excellent sensing towards electrochemical detection of UA. The NiO NPs/CPE show good sensitivity, stability, high linear range, and lower detection limit than in the previous report. The NiO NPs/CPE show high electrocatalytic activity for the anodic peak current of UA. Therefore, the NiO-based electrode is expected to find several applications in sensors, biosensors, and the electrochemistry field.

Conflicts of Interest

The authors declare no conflicts of interest.

Declaration of Funding

The author is thankful to the REVA University, Bangalore, India, through the seed money scheme, file no:RV-IST: PH:2022/08.

REFERENCES

[1] K. M. Dooley, S. Y. Chen, and J. R. H. Ross, J. Catal. 145 (1994) 402.

[2] E. L. Miller, and R. E. Rocheleau, J. Electrochem. Soc. 144 (1997) 3072.

[3] Y. Ichiyanagi, N. Wakabayashi, J. Yamazaki, S. Yamada, Y. Kimishima, E. Komatsu, and H. Tajima, Phys. B: Condens. Matter 329 (2003) 862.

[4] G. Cai, J. P. Tu, J. Zhang, Y. J. Mai, Y. Lu, C. D. Gu, and X. L. Wang, Nanoscale 4 (2012) 5724.
[5] M. Chen, J. Zhang, X. Xia, M. Qi, J. Yin, and Q. Chen, Mater. Res. Bull. 76 (2016) 113.
[6] G. Dryhurst, Electrochemistry of Biological Molecules, Academic Press, New York (1977).
[7] J. Richards, and E. J. Weinman, J. Nephrol. 9 (1996) 160.
[8] P. T. Kissinger, L. A. Pachla, L. D. Reynolds, and S. Wright, J. Assoc. Anal. Chem. 70 (1987) 1.
[9] J. M. Zen, and J. S. Tang, Anal. Chem. 67 (1995) 1892.
[10] H. Yamanaka, R. Togashi, M. Hakoda, C. Terai, S. Kashiwazaki, T. Dan, and N. Kamatani, Adv. Exp. Med. Biol. 431(1998)13.
[11] I. H. Fox, Metabolism. 30 (1981) 616.
[12] Mosby, Manual of Diagnostic and Laboratory Tests (Eds: Pagana, K. Deska), St.Louis, Mosby (1998).
[13] M. H. Alderman, H. Cohen, S. Madhavan, and S. Kivlighn, Hypertension 34 (1999) 144.
[14] L. V. Franse, M. Pahor, M. Di Bari, R. I. Shorr, J. Y. Wan, G. W. Somes, and W. B. Applegate, J. Hypertens. 34 (2000) 1149.
[15] F. Li, T. He, S. Wu, Z. Peng, P. Qiu, and X. Tang, Microchem. J. 164 (2021) 105987.
[16] S. Feng, X. Liu, Chem. Pap. 62 (2008) 318.
[17] T. Hallaj, M. Amjadi, F. Mirbirang, Microchem. J. 156 (2020) 104841.
[18] E. Borras, L. Schrumpf, N. Stephens, B. C. Weimer, C. E. Davis, and E. S. Schelegle, J. Chromatogr. B 1168 (2021) 122588.
[19] Q. Yan, N. Zhi, L. Yang, G. Xu, Q. Feng, Q. Zhang, and S. Sun, Sci. Rep. 10 (2020) 10607.
[20] S. Reddy, B.E. K. Swamy, S. Ramakrishana, L. He, and H. Jayadevappa, Int. J. Electrochem. Sci. 13 (2018) 5748.
[21] J. Gao, P. He, T. Yang, L. Zhou, X. Wang, S. Chen, H. Lei, H. Zhang, B. Jia, and J. Liu, J. Electroanal. Chem. 852 (2019) 113516.
[22] R. A. Soomroa, Z. H. Ibupoto, Sirajuddina, M. I. Abroc, and M. Willander, Sens. Actuators B: Chem. 209 (2015) 966.
[23] S. Reddy, B. E. K. Swamy, S. Aruna, M. Kumar, R. Shashanka, and H. Jayadevappa Chemical Sensors. 2 (2012) 7.
[24] A. S. Chang, A. Tahira, F. Chang, N. N. Memon, A. Nafady, A. Kasry, and Z. H. Ibupoto, RSC Adv. 11 (2021) 5156.